

Supporting Information

Petoukhov et al. 10.1073/pnas.1222000110

SI Text

A.1. Initial Quasibarotropic Vorticity Equation

Here we give a fuller account of the theory of the studied quasiresonance mechanism. We start from a linear nonstationary barotropic vorticity equation on a sphere (1) at the equivalent barotropic level (EBL) (2, 3):

$$\left(\frac{\partial}{\partial t} + \alpha \frac{\partial}{\partial \lambda}\right) \Delta \Psi' + \left(2\Omega - \frac{1}{a \cos \varphi} \Delta \bar{u}\right) \frac{\partial \Psi'}{\partial \lambda} = (\nabla_{\lambda} T' \nabla_{\varphi} \bar{S} - \nabla_{\varphi} \bar{T} \nabla_{\lambda} S') - \frac{2\Omega \sin \varphi \alpha_{or} a^2}{H} \frac{\partial h_{or}}{\partial \lambda} - \left(k_h \frac{\Delta \Psi'}{a^2} + k_z \frac{\Delta \Psi'}{H^2}\right). \quad [\text{S1}]$$

In Eq. S1, t is time; λ is longitude and φ latitude; Ω and a are the earth's rotation angular velocity and radius; Δ , ∇_{λ} , and ∇_{φ} are the horizontal Laplace operator and the longitudinal and meridional components of the gradient operator on a unit sphere, respectively; $\alpha = \frac{\bar{u}}{a \cos \varphi}$ is the atmospheric circulation index; \bar{u} , \bar{T} , and \bar{S} are, respectively, the zonally averaged zonal wind, temperature, and entropy (per unit mass) at the EBL; h_{or} is the large-scale orography height; $\alpha_{or} = \bar{u}_{or}/a \cos \varphi$, where \bar{u}_{or} is the zonal wind at the zonally averaged orography height \bar{h}_{or} (3, 4); T' , Ψ' , and S' are the azonal temperature, stream function, and entropy, respectively, at the EBL; and k_h and k_z are the coefficients of the horizontal and vertical "eddy viscosity," whereas H is the atmospheric density scale height. Taking into account the assumed location of the EBL [500–300 hPa (2, 3)], Eq. S1 can be reduced in the midlatitudes to the quasigeostrophic equation

$$\left(\frac{\partial}{\partial t} + \alpha \frac{\partial}{\partial \lambda}\right) \Delta \Psi' + \left(2\Omega - \frac{1}{a \cos \varphi} \Delta \bar{u}\right) \frac{\partial \Psi'}{\partial \lambda} = \frac{2\Omega \alpha a^2}{\bar{T}} \sin \varphi \frac{\partial T'}{\partial \lambda} - \frac{2\Omega \sin \varphi \alpha_{or} a^2}{H} \frac{\partial h_{or}}{\partial \lambda} - k_h \frac{\Delta \Psi'}{a^2} - k_z \frac{\Delta \Psi'}{H^2}, \quad [\text{S1a}]$$

where \bar{T} is a constant reference temperature at the EBL. We note that the quasibarotropic character of the midlatitude atmospheric circulation in the troposphere during the studied extremes is illustrated clearly by the geographic distribution of the meridional velocity at different pressure levels for the summer 2003 and 2010 heat waves (Fig. S1), as well as for the 1997 Great European Flood and the heat wave in the United States in summer 2011 (Fig. S2).

A.2. Atmospheric Free Wave Solutions

In the case of a zero right-hand side, Eq. S1a describes the adiabatic free atmospheric waves. We are interested in the solutions for the midlatitude free waves. In view of this, it is convenient to use a Mercator projection of the sphere (5) with $x = a\lambda$ and $y = a \ln[(1 + \sin \varphi)/\cos \varphi]$ as new coordinates. After multiplying by $\cos^2 \varphi/a^2$, Eq. S1a in new coordinates takes the form (2)

$$\left(\frac{\partial}{\partial t} + \tilde{u} \frac{\partial}{\partial x}\right) \left(\frac{\partial^2 \Psi'}{\partial x^2} + \frac{\partial^2 \Psi'}{\partial y^2}\right) + \beta \frac{\partial \Psi'}{\partial x} = 0, \quad [\text{S1b}]$$

where $\tilde{u} = \alpha a$ and $\beta = \frac{2\Omega}{a} \cos^2 \varphi - \frac{d}{dy} \frac{1}{\cos^2 \varphi} \frac{d}{dy} (\tilde{u} \cos^2 \varphi)$ is the meridional gradient of the absolute vorticity multiplied by $\cos \varphi$.

The dispersion equation for the free plane wave solutions $\exp i(Kx + ly - \omega t)$ to Eq. S1b reads (2)

$$\omega = \frac{\bar{u}}{\cos \varphi} K - \frac{K}{K^2 + l^2} \left(\frac{2\Omega}{a} \cos^2 \varphi - \frac{d}{dy} \frac{1}{\cos^2 \varphi} \frac{d}{dy} (\cos \varphi \bar{u})\right). \quad [\text{S2}]$$

Eq. S2 does not depend explicitly on x and t . The kinematic wave theory argues that the zonal wave number K and frequency ω in that case are constant on a ray along which the wave energy propagates, and the meridional wave number l varies continuously with latitude such that Eq. S2 holds (6). The variations of l with y are presumed to be small along the ray, with $|dl^{-1}/dy| = o(1)$ everywhere except close to the turning points (TPs) at which $l = 0$ (2). This permits application of the Wentzel-Kramers-Brillouin (WKB) method (7–11) in the classically allowed regions, i.e., outside the vicinity of TPs. In what follows, we consider only the quasistationary waves, with $\omega \approx 0$. For this type of free wave, the magnitude of the group velocity is (6)

$$c_g = 2 \frac{K}{K_s} \tilde{u}, \quad [\text{S3}]$$

where the "stationary wave number" K_s is

$$K_s^2 = \frac{\beta}{\tilde{u}}, \quad [\text{S4}]$$

giving

$$l^2 = \frac{2\Omega \cos^3 \varphi}{a\tilde{u}} - \frac{\cos^2 \varphi}{a^2 \tilde{u}} \frac{d^2 \tilde{u}}{d\varphi^2} + \frac{\sin \varphi \cos \varphi}{a^2 \tilde{u}} \frac{d\tilde{u}}{d\varphi} + \frac{1}{a^2} - \left(\frac{k}{a}\right)^2 \quad [\text{S5}]$$

in terms of $k = Ka$, where k is the nondimensional zonal wave number. For any given k , Eq. S5 determines l^2 as a function of \tilde{u} . l^2 passes through zero value at TPs. In the case of two midlatitude TPs for a free synoptic wave with zonal wave number $k \approx 6-8$, this wave becomes a trapped quasistationary free wave within the latitudinal range (waveguide) confined between the two TPs. This may happen when (i) $\tilde{u} > 0$, $l^2 > 0$ within the waveguide, and $\tilde{u} > 0$, $l^2 < 0$ outside the waveguide; (ii) $|dl^{-1}/ad\varphi| < 1$ within the waveguide's interior; and (iii) the total waveguide's width exceeds the characteristic scale of the relevant Airy function (7–11) for the considered trapped free wave. As shown below, when all three above conditions are met, a quasiresonant amplification of the solution to the fully fledged stationary Eq. S1a with zonal wave number m may occur, provided that (iv) l falls into the range of the meridional wave numbers, which make a dominant contribution to the amplitude of the combined orographic + thermal term on the right-hand side of Eq. S1a in case of $m \approx k$ (section A.3).

A.3. Solutions with Forcing and "Eddy Friction"

As seen from Fig. 3 A–C in the main text, the magnitudes of quasistationary zonal wave numbers $m = 6, 7$, and 8 at 300 hPa were about 4–8 m/s, e.g., in the extreme August 1997, July 2000, August 2003, July 2010, and July 2011. Usually, these waves are much weaker (2, 12, 13). Such a strong magnification may be triggered by the quasiresonance mechanism proposed in our paper. The latter can be investigated with the use of the stationary Eq. S1a with a nonzero right-hand side. Multiplying by $\cos^2 \varphi/a^2$ and projecting to a Mercator plane yields

$$\begin{aligned} \tilde{u} \frac{\partial}{\partial x} \left(\frac{\partial^2 \Psi'}{\partial x^2} + \frac{\partial^2 \Psi'}{\partial y^2} \right) + \beta \frac{\partial \Psi'}{\partial x} = \frac{2\Omega \sin \varphi \cos^2 \varphi}{\tilde{T}} \tilde{u} \frac{\partial T'}{\partial x} \\ - \frac{2\Omega \sin \varphi \cos^2 \varphi}{H} \kappa \tilde{u} \frac{\partial h_{or}}{\partial x} - \left(\frac{k_h}{a^2} + \frac{k_z}{H^2} \right) \left(\frac{\partial^2 \Psi'}{\partial x^2} + \frac{\partial^2 \Psi'}{\partial y^2} \right), \quad [\text{S1c}] \end{aligned}$$

where $\kappa \approx 0.4$ is the characteristic value of the \bar{u}_{or}/\bar{u} ratio (3, 4). In a particular case of midlatitude thermal and orographic terms described by plane waves, $T' = \tilde{T}'_m \cos \frac{m}{a}(x - x_{T,m}) \cos l_{m,y}$ and $h_{or} = h_{or,m} \cos \frac{m}{a} x \cos l_{m,y}$, with zonal wave number m and meridional wave number l_m , the combined orography + thermal term in Eq. S1 may be written for this part of the atmosphere as follows:

$$\begin{aligned} \frac{2\Omega \sin \varphi \cos^2 \varphi}{\tilde{T}} \tilde{u} \frac{\partial T'}{\partial x} - \frac{2\Omega \sin \varphi \cos^2 \varphi}{H} \kappa \tilde{u} \frac{\partial h_{or}}{\partial x} = 2\Omega \sin \varphi \cos^2 \varphi \tilde{u} \frac{m}{a} \\ \times \left[-\frac{\tilde{T}'_m}{\tilde{T}} \sin \frac{m}{a}(x - x_{T,m}) + \kappa \frac{\tilde{h}_{or,m}}{H} \sin \frac{m}{a} x \right] \cos l_{m,y}. \quad [\text{S6}] \end{aligned}$$

In Eq. S6, \tilde{T}'_m and $\tilde{h}_{or,m}$ are the amplitudes of the thermal and orographic terms, respectively, and $x_{T,m}$ is a corresponding longitudinal phase shift between the above-mentioned terms.

We now apply a scale-magnitude consideration (1) to the parameters k_h and k_z in the ‘‘eddy viscosity’’ term $\frac{k_h}{a^2} + \frac{k_z}{H^2}$, which yields

$$\frac{k_h}{a^2} + \frac{k_z}{H^2} = \frac{\tilde{u}L}{a^2} + \frac{\tilde{u}(H\text{Ro})^2}{L H^2}. \quad [\text{S7}]$$

Here, $L \approx (5 \cdot 10^5 - 1 \cdot 10^6)m$ and $\text{Ro} \approx 0.1 - 0.3$ are, respectively, the effective characteristic spatial scale (internal Rossby radius) and Rossby number (1) for the baroclinic eddies contributing to the values of k_h and k_z . When deriving Eq. S7, we follow Stone (1972) (14): the characteristic amplitude of the horizontal velocity in the above eddies nears that of the large-scale zonal wind at their mature stage. We then take into account that the characteristic spatial scale of the longitudinal change of the partial solution Ψ'_m to Eq. S1c for $m = 6 - 8$ is rather small compared with that of the meridional variation of Ψ'_m within the relevant midlatitude waveguides in the course of the considered summer extremes. The total width, $\Lambda_{W,t}$, of the waveguides is about 12.5–15° latitude, and their interior part, Λ_W , with only a weak dependence of l on φ , is about 7.5–10° latitude (section A.4 and Fig. 4). This allows us to neglect, without loss of generality, the $\frac{\partial^2 \Psi'_m}{\partial x^2}$ term in the friction term on the right-hand side of Eq. S1c within Λ_W . Substitution of Eqs. S6 and S7 into Eq. S1c, followed by division by \tilde{u} , results in the following equation for the corresponding m -component of the meridional velocity, v'_m , within Λ_W :

$$\begin{aligned} \frac{\partial^2 v'_m}{\partial x^2} + \frac{\partial^2 v'_m}{\partial y^2} + \left(\frac{L}{a^2} + \frac{\text{Ro}^2}{L} \right) \frac{\partial v'_m}{\partial x} + \frac{\beta}{\tilde{u}} v'_m = 2\Omega \sin \varphi \cos^2 \varphi \frac{m}{a} \\ \times \left[-\frac{\tilde{T}'_m}{\tilde{T}} \sin \frac{m}{a}(x - x_{T,m}) + \kappa \frac{\tilde{h}_{or,m}}{H} \sin \frac{m}{a} x \right] \cos l_{m,y}. \quad [\text{S8}] \end{aligned}$$

We now apply a common approximation used in the description of the combined orographic + thermal term for the Northern Hemisphere (NH) midlatitudes (see, e.g., refs. 3 and 4) that the dominant contribution to this term comes from the meridional wavelengths Λ_d , which range from $\Lambda_{d,1} \approx 60^\circ$ to $\Lambda_{d,2} \approx 70^\circ$ latitude. The respective meridional wave numbers, $l_m = l_d$, in this spectral interval vary between $l_{d,2} = 2\pi/\tilde{\Lambda}_{d,2}$ and $l_{d,1} = 2\pi/\tilde{\Lambda}_{d,1}$, where $\tilde{\Lambda}_{d,i} = \frac{a\Lambda_{d,i}}{\cos \varphi} \frac{\pi}{180^\circ}$ in terms of the Mercator y -coordinate used here (see Eq. S1b and the accompanying text). The above range

of $l_d \approx (0.55 \div 0.66) \cdot 10^{-6} \text{m}^{-1}$ coincides remarkably well with the $l \approx (0.58 \div 0.75) \cdot 10^{-6} \text{m}^{-1}$ obtained for the quasiresonant midlatitude groups of the free waves with $k \approx 6 - 8$ within the interior of all of the waveguides observed in the studied regional extremes (some of these groups are shown in Fig. 4). This suggests that during the extreme months, there existed quasiresonance conditions for the free waves with $k \approx 6 - 8$, not only in a sense of closeness of k to the relevant m -component of the forcing but also in terms of the meridional structure of these waves within the interior of the waveguides, where the range of the resonant l practically coincided with that of l_d . Then, assuming continuous spectra for both l and l_d wave numbers, we can replace l_m by l_d sequentially and substitute l for l_d in Eq. S8. Furthermore, the width of Λ_W is only about $10^{-1}\Lambda_d$ for all the considered waveguides, and the central latitudes, $\varphi_{m,0}$, of the waveguides are located within the range $\varphi_d \approx (40 \div 45)\pi/180$, where the dominant modes, $\tilde{\Lambda}_{d,1}$ to $\tilde{\Lambda}_{d,2}$ of the forcing reach their amplitude values. This means that \tilde{T}'_m/\tilde{T} and $\kappa \tilde{h}_{or,m}/H$ in Eq. S8 can be replaced within the applied WKB approximation by their values, averaged over Λ_W , $(\tilde{T}'_m/\tilde{T})_{W,0}$ and $\kappa(\tilde{h}_{or,m}/H)_{W,0}$, respectively. Also, with an eye to a midlatitude position and the width of Λ_W , we can approximate $\sin \varphi \cos^2 \varphi$ on the right-hand side of Eq. S9 to an accuracy of about 90% by $\sin \varphi_{m,0} \cos^2 \varphi_{m,0}$.

Eq. S8 now may be rewritten as follows:

$$\begin{aligned} \frac{\partial^2 v'_m}{\partial x^2} + \frac{\partial^2 v'_m}{\partial y^2} + \left(\frac{L}{a^2} + \frac{\text{Ro}^2}{L} \right) \frac{\partial v'_m}{\partial x} + \frac{\beta}{\tilde{u}} v'_m = 2\Omega \sin \varphi_{m,0} \cos^2 \varphi_{m,0} \frac{m}{a} \\ \times \left[-\left(\frac{\tilde{T}'_m}{\tilde{T}} \right)_{W,0} \sin \frac{m}{a}(x - x_{T,m}) + \kappa \left(\frac{\tilde{h}_{or,m}}{H} \right)_{W,0} \sin \frac{m}{a} x \right] \cos l_y. \quad [\text{S9}] \end{aligned}$$

We will seek a solution to Eq. S9 in the form

$$v'_m = X_m(x) \cos l_y \quad [\text{S10}]$$

so that $X_m(x)$ obeys the equation

$$\begin{aligned} \frac{d^2 X_m}{dx^2} + \left(\frac{L}{a^2} + \frac{\text{Ro}^2}{L} \right) \frac{dX_m}{dx} + \left(\frac{\beta}{\tilde{u}} - l^2 \right) X_m = 2\Omega \sin \varphi_0 \cos^2 \varphi_0 \frac{m}{a} \\ \times \left[-\left(\frac{\tilde{T}'_m}{\tilde{T}} \right)_{W,0} \sin \frac{m}{a}(x - x_{T,m}) + \kappa \left(\frac{\tilde{h}_{or,m}}{H} \right)_{W,0} \sin \frac{m}{a} x \right]. \quad [\text{S11}] \end{aligned}$$

On the strength of Eq. S5, we can substitute k^2/a^2 for $\beta/\tilde{u} - l^2$ in the left side of Eq. S11, which gives

$$\begin{aligned} \frac{d^2 X_m}{dx^2} + \left(\frac{L}{a^2} + \frac{\text{Ro}^2}{L} \right) \frac{dX_m}{dx} + \frac{k^2}{a^2} X_m \\ = 2A_m^{\text{Ort}} \Omega \sin \varphi_0 \cos^2 \varphi_0 \sin \left(\frac{m}{a} x + x_m^{\text{Ort}} \right), \quad [\text{S12}] \end{aligned}$$

where k is a constant longitudinal wave number of the decelerated free wave trapped within the relevant waveguide, whereas the amplitude A_m^{Ort} and phase x_m^{Ort} of the combined orographic and thermal forcing obey

$$\begin{aligned} A_m^{\text{Ort}} = \left(m/a \right) \text{sqrt} \left(A^2 + B^2 + 2AB \cos \frac{m}{a} x_{T,m} \right), \\ x_m^{\text{Ort}} = A \tan \left(\tilde{B}/\tilde{A} \right). \quad [\text{S13}] \end{aligned}$$

In Eq. S13, $A = (\tilde{T}'_m/\tilde{T})_{W,0}$, $B = -\kappa(\tilde{h}_{or,m}/H)_{W,0}$, $\tilde{A} = A \cos(mx_{T,m}/a) + B$, and $\tilde{B} = -A \sin(mx_{T,m}/a)$.

Eq. S12 is a classical nonhomogeneous linear equation with constant parameters, describing a quasiresonant behavior of

the variable X_m subjected to periodic force. Its solution may be written as follows:

$$X_m = \tilde{A}_m^{Ort} 2\Omega \sin \varphi_0 \cos^2 \varphi_0 \frac{\sin\left(\frac{m}{a}x + x_m^{Ort} - \gamma_m\right)}{\left\{ \left[\frac{k^2}{a^2} - \frac{m^2}{a^2} \right]^2 + \left[\frac{L}{a^2} + \frac{Ro^2}{L} \right]^2 \left(\frac{m}{a} \right)^2 \right\}^{1/2}} \quad [\text{S14}]$$

so that the amplitude of v'_m yields

$$\tilde{A}_m = \tilde{A}_m^{Ort} \frac{2\Omega \sin \varphi_{m,0} \cos^2 \varphi_{m,0}}{\left\{ [K^2 - M^2]^2 + (L/a^2 + Ro^2/L)M^2 \right\}^{1/2}}, \quad [\text{S15}]$$

where $K = k/a$ and $M = m/a$. The zonal phase shift γ_m of v'_m relative to the orographic forcing in Eq. S14 yields

$$\gamma_m = \frac{1}{M} A \tan \left\{ \frac{\left(\frac{L}{a^2} + \frac{Ro^2}{L} \right) M}{K^2 - M^2} \right\}. \quad [\text{S16}]$$

On the strength of Eq. S15, the amplitude \tilde{A}_m of v'_m may reach a very high quasiresonance value within the waveguide's interior for a particular wave number $m = 6 - 8$ in the case of $k \rightarrow m$. The parameters of the orographic and thermal terms on the right-hand side of Eq. S13, $(\tilde{h}_{or,m})_{W,0}$, $(\tilde{T}'_m)_{W,0}$, and $x_{T,m}$, have been calculated based on the observational data from refs. 15 and 16 (section A.5).

Away from Λ_W , the amplitude \tilde{A}_m of the solution v'_m for the quasiresonance waves is described by the Airy function (2, 7–9) (see also section A.4). This function is wavelike within the waveguides and evanescent otherwise. With the use of this function, a lateral boundary condition of monotonic decay of the solution for v'_m outside the waveguides is satisfied (7–11).

Based on Eq. S5, quasiresonance conditions $i-iv$ held for the synoptic wave numbers $k \approx 6 - 8$ in the appropriate waveguides during the most destructive phases of the regional summer extremes. These extremes are listed in section A.6. We performed calculations of the midlatitude amplitudes, $\langle \tilde{A}_m \rangle$, of v'_m in the (37.5–57.5)°N latitudinal belt at 300 hPa for the wave numbers $m = 6, 7$, and 8 during these most destructive phases of extremes. $\langle \tilde{A}_m \rangle$ is a result of the latitudinal averaging over the indicated latitudinal belt of the values of \tilde{A}_m , described by the solution to Eq. S15 within the interiors of the corresponding waveguides, and by the aforementioned Airy function outside Λ_W . Our calculations show that July 31 to August 14, 2003, was characterized by $\langle \tilde{A}_7 \rangle \approx 8.0$ m/s, and wave 6 and wave 7 patterns had the amplitudes $\langle \tilde{A}_6 \rangle \approx 7.7$ m/s and $\langle \tilde{A}_7 \rangle \approx 5.4$ m/s, respectively, in August 4–13, 2002. The period July 8–22, 2011, in the course of the severe heat wave in the United States featured $\langle \tilde{A}_6 \rangle \approx 9.0$ m/s, and July 25 to August 7, 2010, during the Russian heat wave was characterized by $\langle \tilde{A}_6 \rangle \approx 6.5$ m/s and $\langle \tilde{A}_7 \rangle \approx 5.8$ m/s. Analogous calculations confirm that the most devastating period of the Great Flood in Europe, from June 25 to July 4, 1997, and the catastrophic period of the floods in the Tisza basin, northern Italy and eastern Europe, between July 10 and 26, 2000, exhibited, accordingly, $\langle \tilde{A}_8 \rangle \approx 7.1$ m/s and $\langle \tilde{A}_7 \rangle \approx 8.2$ m/s. By comparison, the corresponding Fourier components calculated directly from daily National Centers for Environmental Prediction–National Center for Atmospheric Research reanalysis data (16) had amplitudes of about 7.3 m/s for $m = 7$ from July 31 to August 15, 2003; 7.2 m/s for $m = 6$ and 4.8 m/s for $m = 7$ from August 4–13, 2002; 8.3 m/s for $m = 6$ from July 8–22, 2011; 5.8 m/s for $m = 6$ and 5.0 m/s for $m = 7$

from July 25 to August 7, 2010; 6.5 m/s for $m = 8$ from June 25 to July 7, 1997; and 7.1 m/s for $m = 7$ during July 10–26, 2000.

Similar estimations were conducted for monthly amplitudes $\langle \tilde{A}_m^{mon} \rangle$ of the quasiresonant wave numbers $m = 6 - 8$ over the (37.5–57.5)°N belt during the extreme months listed in section A.6. As an example, the calculated monthly $\langle \tilde{A}_7^{mon} \rangle$ is about 4.8 m/s for August 2003, $\langle \tilde{A}_7^{mon} \rangle$ reaches 4.1 m/s for August 2004, $\langle \tilde{A}_8^{mon} \rangle$ ranges up to 2.6 m/s for July 1993, $\langle \tilde{A}_6^{mon} \rangle$ runs as high as 4.7 m/s for July 1994, and $\langle \tilde{A}_6^{mon} \rangle$ amounts to up to 6.1 m/s for August 1983. The respective amplitudes computed directly from daily reanalysis data (16) are as follows (Fig. 3 A–C): $\langle \tilde{A}_7^{mon} \rangle \approx 4.2$ m/s for August 2003, $\langle \tilde{A}_7^{mon} \rangle \approx 3.6$ m/s for August 2004, $\langle \tilde{A}_8^{mon} \rangle \approx 2.1$ m/s for July 1993, $\langle \tilde{A}_6^{mon} \rangle \approx 4.1$ m/s for July 1994, and $\langle \tilde{A}_6^{mon} \rangle \approx 5.3$ m/s for August 1983.

At the same time, according to our calculations of l^2 with the use of Eq. S5, most of the Julys and Augusts (31 mo) over the 1980–2011 time interval, with low and intermediate amplitudes of all three wave numbers $m = 6, 7, 8$, as well as the 1980–2011 climatology of $\bar{u}(\varphi)$, exhibit only one midlatitude TP for corresponding $k \approx 6 - 8$. For the remainder of months with low and intermediate amplitudes for all of the above wave numbers (13 mo), with two TPs, at least one of requirements $i-iv$ was not met: in particular, according to Eq. S5, the values of l in the corresponding free waves for these months were below $0.4 \cdot 10^{-6} \text{m}^{-1}$. This prevented a development of waveguides for all these months and the 1980–2011 climatology, thus making solution S15 to Eq. S8 not applicable in these cases.

A.4. Checking Procedure for Quasiresonant Requirement iii

For the validity of the WKB approach applied in our study, it is necessary, in particular, for the waveguide's width to exceed the characteristic spatial scale $\Delta\varphi_A$ for the wavelike branch of the relevant Airy function (2, 7–11) in the vicinity of the corresponding TP (waveguide's lateral boundary) within the waveguide for the decelerated free waves (section A.2). $\Delta\varphi_A$ may be written as $\frac{\Lambda_A}{4\pi}$ (7–11), where Λ_A is the characteristic wavelength of the Airy function. In terms of the width of the corresponding latitudinal strip $\Delta\varphi_A$ this yields

$$C_1^{1/3} \Delta\varphi_A \approx 1/\pi, \quad [\text{S17}]$$

where

$$C_1 = |dF(\varphi)/d\varphi|_{TP}. \quad [\text{S18}]$$

In Eq. S18, $|dF(\varphi)/d\varphi|_{TP}$ is the modulus of the first derivative with respect to φ of the function $F(\varphi) = a^2 l^2(\varphi)/\cos^2 \varphi$, at TP. According to Eq. S17, Eq. S18 $\Delta\varphi_A$ is about 2.25–3.75° latitude for the waveguides considered in our paper.

Notably, the validity of the WKB approach strongly depends on the width of the considered latitudinal range. The latter should be located in midlatitudes and must not be too wide. This is necessary, to avoid combining zonal means [e.g., $\bar{u}(\varphi)$] from latitudes with noticeably different numbers of independent observations/reanalysis data (degrees of freedom) used to compute these zonal means. As shown in ref. 17, this may bring about misleading results when comparing different climate states and scenarios. The position and width of the midlatitude range, (30 ÷ 60)°N, that we have chosen for our study allow us to circumvent this difficulty.

A.5. Calculation of the Parameters of the Combined Orographic and Thermal Forcing and Its Temporal Variability

The parameters of the orographic and thermal forcing, $(\tilde{h}_{or,m})_{W,0}$, $(\tilde{T}'_m)_{W,0}$, and $x_{T,m}$, were computed applying the Fourier decomposition to the longitudinal distribution of the averaged over Λ_W orography height $(h_{or})_{W,0}$ and monthly or 15-d means of the azonal temperature $(T')_{W,0}$. The calculated magnitudes

$(\tilde{h}_{or,m})_{W,0}$ and $(\tilde{T}'_m)_{W,0}$ of the combined forcing with zonal wave numbers $m=6, 7$, and 8 , as well as the longitudinal phase shift $x_{T,m}$ between the two components of forcing were then substituted into the right side of Eq. S13 to obtain the parameters of the combined forcing.

We estimated the role of the intrinsic natural year-to-year variability of the combined term in Eq. S15 compared with its 1980–2011 climatology, for Julys and Augusts, within the $(37.5\text{--}47.5)^\circ\text{N}$ range common to the position and width of Λ_W . For this purpose, we first calculated the absolute value $|\Delta M_{N,i}|$ of the difference between the magnitudes of the combined term for a given N -th month (where $n = 1, \dots, 64$) and the corresponding 1980–2011 climatology, for each i -th 2.5° latitudinal strip (where $i = 1, \dots, 4$) within the indicated 10° latitudinal range. For these calculations, we applied the formulas from Eq. S13 for a given month within each strip. Then for each strip, we normalized $|\Delta M_{N,i}|$ by the magnitude $|M_i|$ of the 1980–2011 climatology of the forcing. The obtained ratios, $|\Delta M_{N,i}|/|M_i|$, were then weighted over the total $(37.5\text{--}47.5)^\circ\text{N}$ range, for a given N -th month. We used as a weighting factor the product $\cos \varphi_i |M_{N,i}|$, where $|M_{N,i}|$ is the absolute value of the forcing in the i -th strip for a given month. We conducted these calculations for each wave number $m=6, 7$, and 8 . The results of the calculations are shown in Fig. S4A for Julys and Fig. S4B for Augusts. The calculations attest that the magnitude, $\tilde{A}_{m,v}^{Ort}$, of the year-to-year variability of \tilde{A}_m^{Ort} normalized by its 1980–2011 climatology, $\tilde{A}_{m,cl}^{Ort}$, was less than 20% in the $(37.5\text{--}47.5)^\circ\text{N}$ belt for all $m=6, 7$, and 8 in most Julys, except July 1980 ($\tilde{A}_{6,v}^{Ort} \approx 22.5\%$), July 1985 ($\tilde{A}_{6,v}^{Ort} \approx 27\%$), and July 2003 ($\tilde{A}_{6,v}^{Ort} \approx 25\%$) (section A.5 and Fig. S4A). During Augusts, $\tilde{A}_{m,v}^{Ort}$ did not exceed 17% for all three wave numbers m , except for August 1984 ($\tilde{A}_{6,v}^{Ort} \approx 36\%$), August 1994 ($\tilde{A}_{6,v}^{Ort} \approx 25\%$), and August 2010 ($\tilde{A}_{6,v}^{Ort} \approx 33\%$ and $\tilde{A}_{8,v}^{Ort} \approx 25\%$) (section A.5 and Fig. S4B). None of the above Julys is the quasiresonant extreme month for all three wave numbers $m=6, 7$, and 8 (Fig. 3A–C), and only August 1984 is among the quasiresonant extreme Augusts for $m=6$ (Fig. 3A). This means that the main contribution to strong amplification (factor of 3–4) of the amplitudes of the above wave numbers during the months with studied regional extremes, except maybe August 1984, does not result from intrinsic natural variability, but rather from the considered quasiresonance mechanism.

A.6. Brief Description of the Considered Record Regional Extremes

In this paper, we performed a statistical analysis of the magnitudes of the quasistationary midlatitude planetary waves in the NH with high (synoptic-scale) zonal wave numbers $m=6\text{--}8$ over the 1980–2011 time span, for Julys and Augusts. We showed that very high amplitudes of these waves occurred during the months characterized by severe regional heat waves and destructive floods in the NH midlatitudes. These latter months are as follows in the inverse chronological order, with the phase of El Niño–Southern Oscillation (ENSO) indicated in parentheses to demonstrate rather weak dependence of the chronology of the extremes on the ENSO phase (see www.heatisonline.org/contentserver/

objecthandlers/index.cfm?id=3357&method=full and <http://ggweather.com/enso/oni.htm>, where the appropriate references are given to the sources of the information shown below):

July 2011: record heat wave in the United States, resulting in the fourth warmest July on record nationally and the driest conditions in the southern United States ever (weak summer La Niña)

July/August 2010: Russian heat wave and the Pakistan flood, with the strongest and most persistent extreme weather conditions and the highest death tolls from heat waves and floods ever for these two regions (strong summer La Niña)

July 2006: temperatures higher than 100°F for only the second time in Britain's history and much of Europe experiencing a serious heat wave (weak summer El Niño)

August 2004: much of northern Europe hit by very low winter-like temperatures and sporadic snowfalls (moderate to strong summer El Niño)

August 2003: European summer 2003 heat wave, causing a highly persistent drought in western Europe (weak summer El Niño)

August 2002: catastrophic Elbe and Danube floods (strong summer El Niño)

July 2000: destructive floods in northern Italy and the Tisza basin and a simultaneous heat wave in the southern United States, smashing all-time high-temperature records by that time at many sites (strong summer La Niña)

July/August 1997: disastrous Great European Flood, which caused several deaths in central Europe, and the destroying floods in Pakistan and western United States (strong summer El Niño)

July 1994: very strong heat wave in southern Europe, with a national temperature record of 47.2°C set in Spain (weak summer El Niño)

July 1993: unprecedented great flood in the United States that reigned over the country from April (weak summer El Niño)

July 1989: unusually intense and unprecedented widespread drought in the United States (weak summer La Niña)

August 1987: severe drought in the southeastern United States (strong summer El Niño)

August 1984: continuation of the severe heat of summer 1983, with serious drought in the United States (weak summer La Niña)

July and August 1983: very dry conditions, severe heat, and substandard crop growth (5–35% below normal) in the mid-western United States (weak summer El Niño)

Of special note: June, July, and early August 2012 (Fig. S3) featured catastrophic floods in China and Japan, as well as record-breaking temperatures during heat waves in the United States and southern Europe (weak summer El Niño).

- Pedlosky J (1979) *Geophysical Fluid Dynamics* (Springer, New York).
- Hoskins BJ, Karoly DJ (1981) The steady linear response of a spherical atmosphere to thermal and orographic forcing. *J Atmos Sci* 38:1179–1196.
- Charney JG, Eliassen A (1949) A numerical method for predicting the perturbations of the middle latitude westerlies. *Tellus* 1:39–54.
- Held IM (1983) Stationary and quasi-stationary eddies in the extratropical troposphere: Theory. *Large-Scale Dynamical Processes in the Atmosphere*, eds Hoskins BJ, Pearce RP (Academic, London), pp 127–168.
- Phillips NA (1973) Principles of large-scale numerical weather prediction. *Dynamical Meteorology*, ed Morel P (Reidel, Dordrecht, the Netherlands), pp 3–96.
- Whitham GB (1960) A note on group velocity. *J Fluid Mech* 9:341–352.
- Dingle RB (1973) *Asymptotic Expansions: Their Derivations and Interpretation* (Academic, London).
- Murdock JA (1991) *Perturbations. Theory and Methods* (Wiley, New York).

- Heading J (1962) *An Introduction to Phase Integral Methods* (Wiley, New York).
- Olver FWJ (1975) Second-order linear differential equations with two turning points. *Phil Trans Roy Soc* 278(1279):137–174.
- Matkowsky BJ (1975) On boundary layer problems exhibiting resonance. *SIAM Rev* 17:82–100.
- Eliassen E, Machenhauer B (1965) A study of the fluctuations of the atmospheric planetary flow patterns represented by spherical harmonics. *Tellus* 17:220–238.
- Petri S (2012) Supplementary material for quasiresonant amplification of planetary waves and recent Northern Hemisphere weather extremes. Available at www.pik-potsdam.de/~petri/planwaveresonance.html.
- Stone PH (1972) A simplified radiative-dynamical model for the static stability of rotating atmospheres. *J Atmos Sci* 29:405–418.

15. Hastings DA, Dunbar PK (1999). Global land one-kilometer base elevation (GLOBE) digital elevation model, Documentation, Volume 1.0. Key to Geophysical Records Documentation (KGRD) 34. (National Oceanic and Atmospheric Administration, National Geophysical Data Center, Boulder, CO).

16. Kalnay E, et al. (1996) The NCEP/NCAR 40-year reanalysis project. *Bull Am Meteorol Soc* 77:437-470.

17. Benestad RE (2005) On latitudinal profiles of zonal means. *Geophys Res Lett* 32: L19713.

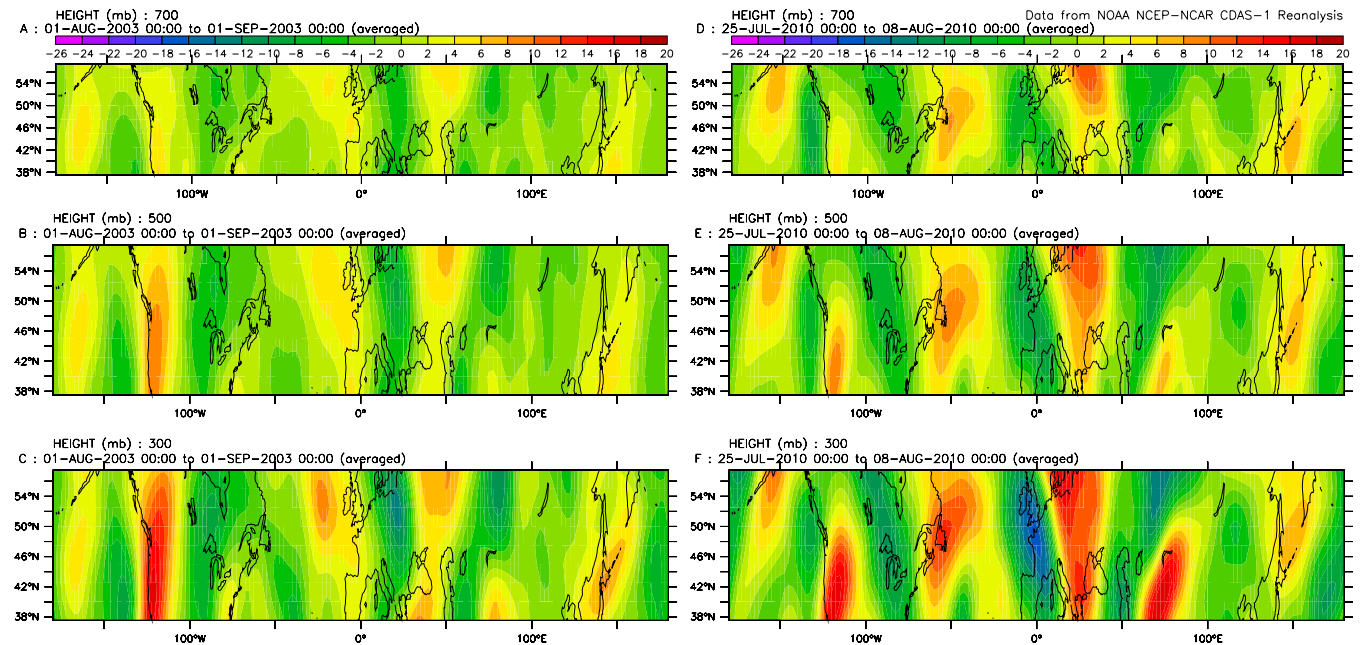


Fig. S1. Vertical distributions of the midlatitude meridional velocity (in meters per second) for mean August 2003 and July 25 to August 7, 2010. Images show the corresponding variable at 700 hPa (A and D), 500 hPa (B and E), and 300 hPa (C and F) levels for August 2003 (Left) and July 25 to August 7, 2010 (Right).

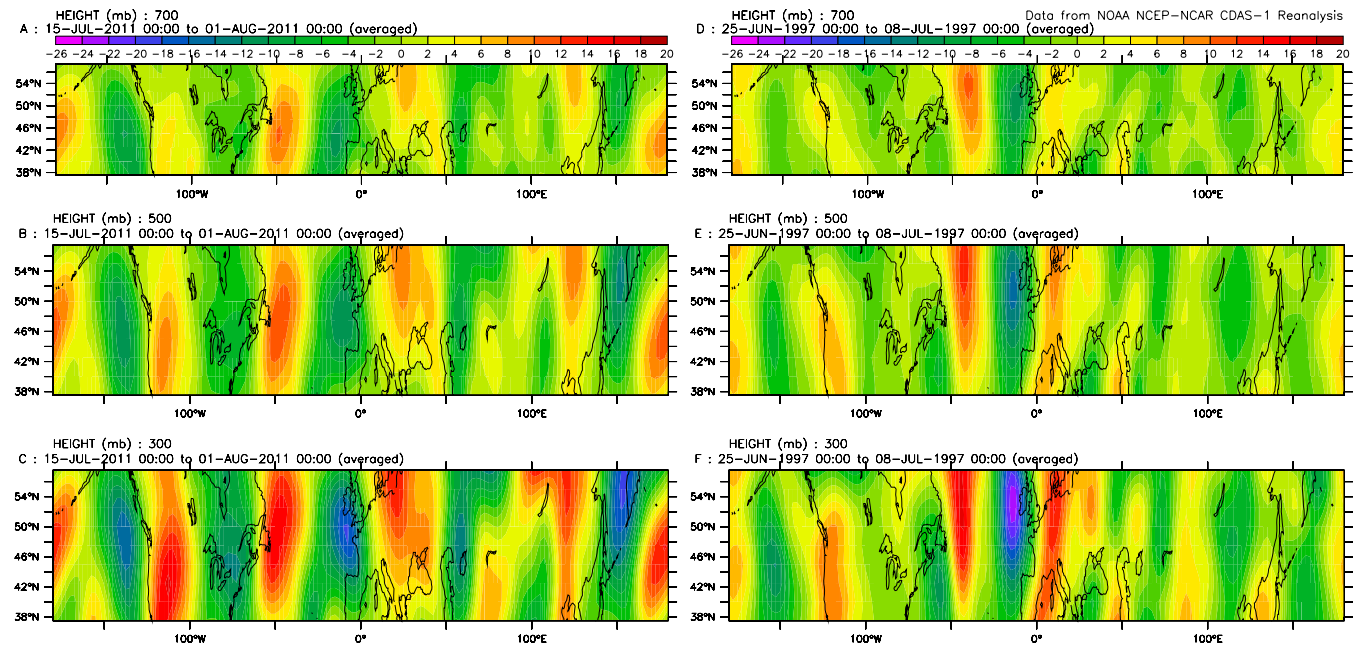


Fig. S2. Same information as in Fig. S1, but for July 15 to 31, 2011, and June 25 to July 7, 1997. Images show the corresponding variable at 700 hPa (A and D), 500 hPa (B and E), and 300 hPa (C and F) levels for August 15 to 31, 2011 (Left), and June 25 to July 7, 1997 (Right).

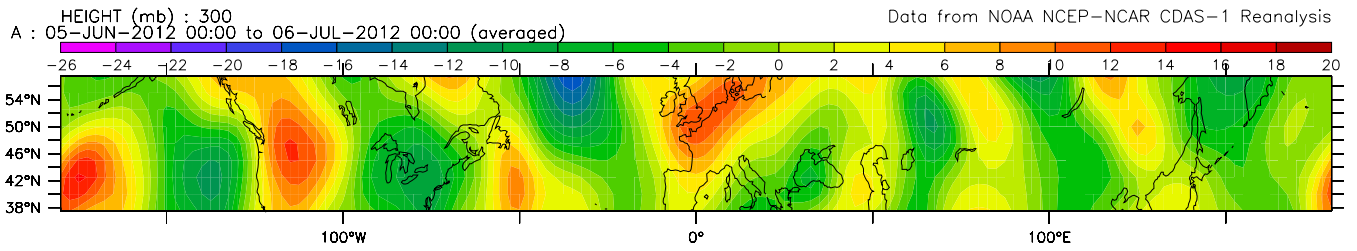


Fig. S3. Map of the meridional winds (in meters per second) at 300 hPa over the North Atlantic–European midlatitude sector averaged over the period from June 6 to July 6, 2012, during destructive heat waves in the United States and southern Europe and catastrophic floods in China and Japan.

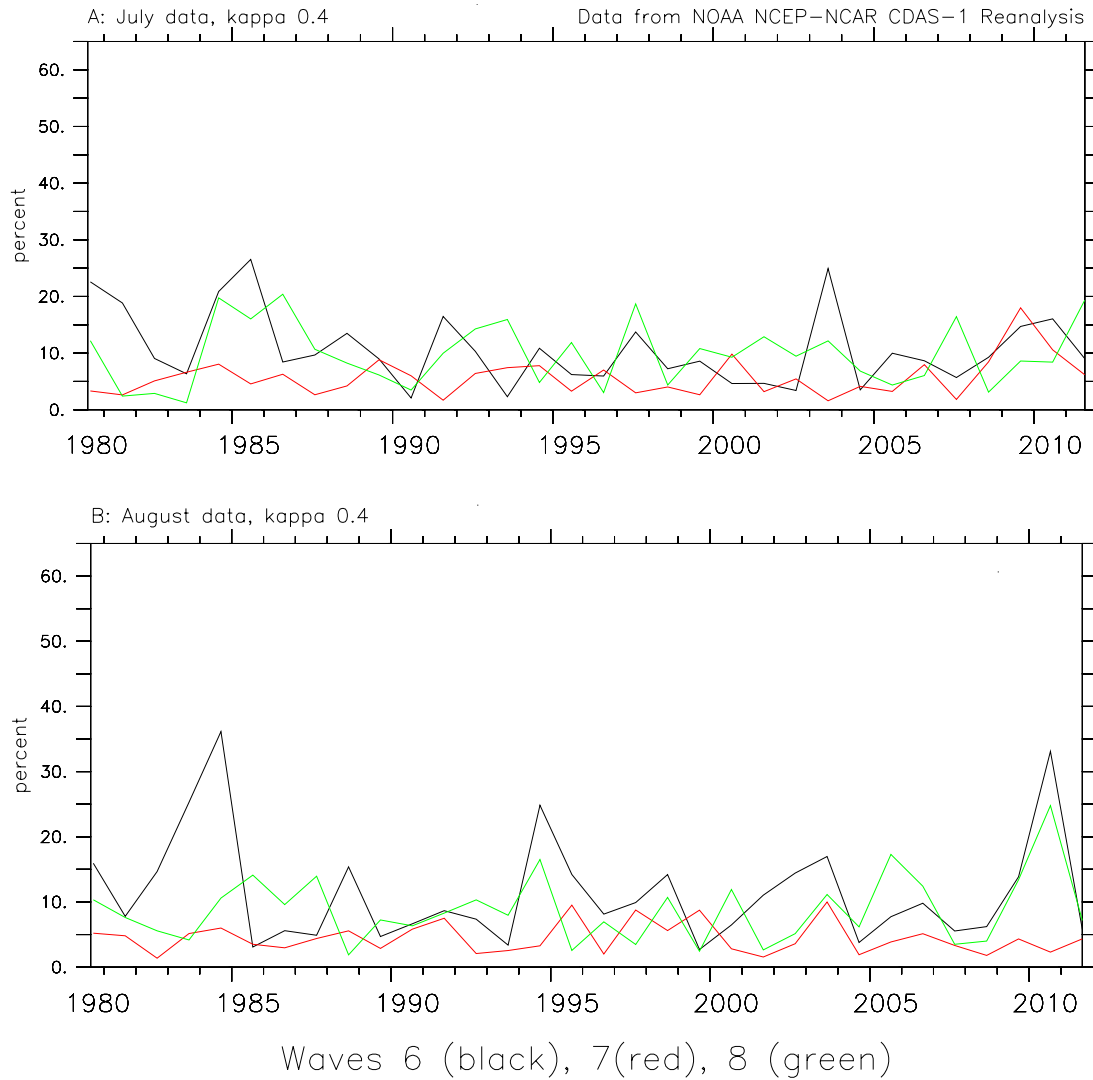


Fig. S4. (A) Magnitude, $\bar{A}_{m,v}^{Ort}$ (in percent), of the year-to-year variability over the 1980–2011 time span of the combined orographic and thermal forcing \bar{A}_m^{Ort} in the (37.5–47.5)°N latitudinal range, normalized by the 1980–2011 climatology of \bar{A}_m^{Ort} , for Julys. $\bar{A}_{m,v}^{Ort}$ is shown for the wave numbers $m=6$ (black), $m=7$ (red), and $m=8$ (green). (B) Same information as in A, but for Augusts.